Published in final edited form as:
J Mol Cell Cardiol. 2008 November ; 45(5): 642–649. doi:10.1016/j.yjmcc.2008.08.013.

Decreased intercellular coupling improves the function of cardiac pacemakers derived from mouse embryonic stem cells

John P. Fahrenbach[1], **Xun Ai**[2], and **Kathrin Banach**[3]

1 *Department of Physiology, Stritch School of Medicine, Loyola University Chicago, Maywood, IL, USA*

2 *Division of Cardiovascular Disease, University of Alabama at Birmingham, 1670 University Blvd, Birmingham, AL 35294-0019*

3 *Center for Cardiovascular Research, Dept. of Medicine, Section of Cardiology, University of Illinois at Chicago, Chicago, IL, USA*

Abstract

The aim of this study was to determine if embryonic stem cell-derived cardiomyocyte aggregates (ESdCs) can act as pacemakers in spontaneously active cardiomyocyte preparations when their connexin isoform expression is tuned toward a more sinus nodal phenotype. Using microelectrode array recordings (MEAs), we demonstrate that mouse ESdCs establish electrical coupling with spontaneously active cardiomyocyte preparations (HL-1 monolayer) and obtain pacemaker dominance. WT- and Cx43(−/−)-ESdCs comparably established intercellular coupling with cardiac host tissue (Cx43(−/−): 86 % vs. WT: 91 %). Although both aggregates had a 100 % success rate in pacing quiescent cardiac preparations, Cx43(−/−)-ESdCs had an increased likelihood of gaining pacemaker dominance (Cx43(−/−): 40 % vs. WT: 13 %) in spontaneously active preparations. No differences in size, beating frequency, V_m, or differentiation were detected between WT- and Cx43(−/−)-ESdCs but the intercellular coupling resistance in Cx43(−/−)-ESdCs was significantly increased (Cx43(−/−): 1.2 nS vs. WT: 14.8 nS). Lack of Cx43 prolonged the time until Cx43(−/−)-ESdCs established frequency synchronization with the host tissue. It further hampered the excitation spread from the cardiomyocyte preparation into the ESdC. However rectifying excitation spread in these co-cultures could not be unequivocally identified. In summary, ESdCs can function as dominant biological pacemakers and Cx43 expression is not a prerequisite for their electrical integration. Maintenance of pacemaker dominance depends critically on the pacemaker's gap junction expression benefiting those with increased intercellular coupling resistances. Our results provide important insight into the design of biological pacemakers that will benefit the use of cardiomyocytes for cell replacement therapy.

Introduction

The use of artificial pacemakers in the treatment of sinoatrial node (SAN) dysfunction and conduction abnormalities is well established; however, their limited neurohumoral responsiveness and surgically invasive repair argues for the development of maintenance-free biological pacemakers. Different approaches have been pursued to develop biological

Corresponding Author: Kathrin Banach, Ph.D., Section of Cardiology, Department of Medicine, University of Illinois at Chicago, 840 South Wood Street (MC 715), Chicago, Illinois 60612-7323, Phone: 312 996 5018, e-mail: kbanach@uic.edu.

pacemakers using cell replacement therapy including the transplantation of isolated spontaneously active fetal cardiomyocytes [1] or embryonic stem cell derived cardiomyocyte (ESdC) aggregates [2,3]. Though these approaches yield promising results, they only focus on inducing spontaneous activity which is necessary but not sufficient for a functional biological pacemaker. Spontaneous activity in pacemaker cells also depends on their intercellular coupling with host myocardium. The intercellular coupling established in the SAN and in the transition from SAN to atrial cardiomyocytes plays a crucial role in the stability and dominance of this physiological pacemaker [4–6]. The major gap junction isoforms expressed in the murine SAN cardiomyocytes are Cx45 [7] and Cx30.2 [8]. These connexin isoforms establish low conductance gap junction channels which result in a high intercellular resistance between SAN cardiomyocytes and between SAN and atrial or translational cardiomyocytes [6]. This working hypothesis is supported by a “pacemaker model” that demonstrates increased intercellular resistance protects the SAN cells from hyperpolarization [9] or slowing and eventually quiescence of the pacemaker rhythm [10,11]. In addition to the intercellular resistance, the voltage dependent gating of gap junction channels is believed to play a role in pacemaker function. The heterogeneous expression of connexin isoforms in the SAN and the atrial muscle cells favors the formation of heterotypic gap junction channels at the site of heterocellular interaction [5]. Possible gap junction channels in this area would be heterotypic combinations of Cx45/Cx40, Cx45/Cx43 [12] as well as Cx30.2/Cx40 and Cx30.2/Cx43 [8]. All potential heterotypic combinations establish intercellular junctions that exhibit rectifying voltage dependent gating properties as demonstrated in unexcitable heterologous expression systems [8,12]. It is hypothesized that these rectifying junctions would favor AP propagation from the SAN to the atrial muscle which may prevent the suppression of SAN excitation by ectopic arrhythmic stimuli.

Embryonic stem cells (ESC) are widely discussed as a potential source for cardiac replacement tissue. The cells differentiate *in vitro* into multicellular cardiomyocyte aggregates (ESdCs) that exhibit spontaneous electrical activity [13,14]. ESdCs recapitulate the early embryonic development of the cardiac tissue also in regards to the expression of gap junction isoforms Cx40, Cx43 and Cx45 [14,15]. Aggregates of human ESdCs have been shown to act as biological pacemakers by entraining host cardiomyocyte preparations *in vitro* and *in vivo* after transplantation [2,3]. In these studies, the spontaneous activity of the host tissues was eliminated by ablation of the SAN or atrio-ventricular node (AVN) respectively, which allowed the ESdCs to obtain pacemaker dominance.

In this study, we determined that ESdC aggregates can obtain pacemaker dominance in the presence of ectopic spontaneous activity and that the modulation of ESdC gap junction isoform expression towards a more SAN phenotype, namely the lack of Cx43 expression, significantly increased pacemaker dominance of the ESdCs in spontaneously active preparations.

Materials and Methods

Cell culture of HL-1 cells and mouse ESCs

HL-1 cells, a cardiac muscle cell line derived from the mouse atrial cardiomyocyte tumor lineage AT-1 were cultured as previously described [16,17] in Claycomb media (JRH Bioscience) supplemented with fetal bovine serum (FBS) (10 %), L-glutamine (2 mM), and norepinephrine (0.1 mM). To obtain monolayers of spontaneously active cells, HL-1 cells were plated at 4×10^5 cells/ml on microelectrode arrays (MEA). The cells reached confluence and exhibited synchronized spontaneous activity after 1 day in culture [18]. HL-1 cells displayed an atrial like phenotype in terms of their action potential and exhibited homogeneous excitation spread when they established monolayers on MEAs (see Fig. S1A) [16,17]. To attain quiescent HL-1 monolayers, FBS in the media was reduced to 2 % and norepinephrine was withdrawn from the HL-1 culture media while the HL-1 cells were maintained [19]

ESCs of the cell line (D3), and Cx43(−/−) [13,18,20,21] were propagated in culture and differentiated as embryoid bodies (EBs) [13,22]. In plated EBs, spontaneously beating aggregates of cardiomyocytes were observed after 8 days of culture. The beating frequency increased with time in culture and stabilized in both cell lines (see Fig. S3A,B) after ~14 days [13]. At this time, ESdCs were microdissected from EBs and transferred onto monolayers of HL-1 cells growing on MEAs. During all MEA measurements cells were maintained in HEPES buffered Claycomb media.

MEA recordings and analysis

We used substrate integrated, planar MEAs (Multi Channel Systems, Reutlingen, Germany) for recordings of field potentials (FPs) originating from the spontaneous electrical activity of HL-1 cells and ESdCs [13,22,23]. MEAs consisted of 60 Titanium Nitride coated gold electrodes (Ø = 30 μm; inter-electrode distance 200 μm in a square grid) with an integrated ground electrode. The MEA was connected to an amplifier and data acquisition system, which included a heating device to maintain a constant temperature of 37°C (Multi Channel System, Reutlingen, Germany). The data were analyzed off-line with a customized toolbox programmed for MATLAB (The Mathworks, Natick, MA, USA) [23,24].

Western blot

Western blotting was performed to assess the protein expression using specific antibodies to Cx40 (Santa Cruz), Cx43 (Chemicon), Cx45 (Zymed) as previously described [25]. In brief, differentiated and microdissected WT- and Cx43(−/−)-ESdC aggregates were homogenized in RIPA buffer containing a protease inhibitor cocktail (Sigma). Protein content was quantified using a DC protein assay kit (Bio-Rad). Cell lysates (containing of 40 μg protein) were separated by a 10 % SDS-PAGE gel and transferred onto a nitrocellulose membrane. Then the transferred membrane was incubated with a primary antibody overnight at 4°C, followed by 2-hour incubation with a peroxidase-conjugated secondary antibody. Immunoreactivity was detected by chemiluminescence (ECL Western Blotting Analysis System, Amersham). Equal protein loading of the gels was assessed by re-probing the membrane with monoclonal anti-GAPDH antibody (Chemicon). Immunostainings were performed as previously described [18]. The Cx30.2 antibody was provided by Dr. N. Kumar (UIC, Chicago, IL; [26]). ESdCs were double stained with α-actinin to confirm their cardiac phenotype.

Results

ESdCs establish electrical coupling with the host preparation

The success rate of ESdCs in obtaining pacemaker dominance was almost 100 % *in vitro* in quiescent cardiomyocyte preparations of neonatal rat cardiomyocytes and *in vivo* in SAN or AVN ablated pigs and dogs, respectively [2,3]. To address the question of whether ESdCs are able to obtain pacemaker dominance during spontaneous activity in a cardiac host tissue, we transplanted ESdCs onto cardiomyocyte monolayers of HL-1 cells. ESCs differentiate in culture into spontaneously beating aggregates of cardiomyocytes. Comparable to our previous studies [13,27], WT-ESdCs established a stable beating frequency of 1.3 ± 0.1 Hz (n = 8 cultures) after 7 days on the MEA (14 days old). Micro-dissected ESdCs (14–18 days old) plated on MEAs retained the frequency observed in the EB preparation (1.1 ± 0.4 Hz; n = 5) and were used for the ESdC/HL-1 co-cultures. Under optical control, we positioned isolated ESdC aggregates in the center of the MEA electrode field onto HL-1 monolayers and monitored online the spontaneous activity of both preparations while heterocellular coupling was established. Figure 1A shows a representative field potential recording from a single MEA electrode. This electrode was located underneath the ESdC and records the spontaneous activity of the HL-1 cells and the ESdC. The spontaneous activity of the HL-1 cell monolayer is

represented in the large negative spikes (3.1 ± 0.05 Hz) whereas the ESdC spontaneous activity is represented in the smaller, less frequent negative spikes (1.4 ± 0.1 Hz) marked by the arrows.

In the first phase of co-culture, the inter-spike interval (ISI) of all recorded spikes is non-stationary (Fig. 1B (i)). Separate analysis of the 2 different spike waveforms reveals two constant ISIs whose values are comparable to the characteristic frequencies of individual HL-1 and ESdC preparations respectively (Fig. 2C). The time delay between these two different waveforms in a single excitation cycle varies continuously supporting the electrical independence of the two preparations (Fig. 2A (i), B). As co-culture progressed (Fig. 1AB (ii); 28 min), the plot of the ISIs against time becomes more ordered and the delay between HL-1 and ESdC spikes stabilizes transiently (Fig. 2AD). In the case shown, the ESdC's ISI (Fig. 2E) becomes an integral value of the HL-1's ISI suggesting that heterocellular coupling has been established and action potential (AP) propagation between the two preparations happens in 1 out of 2 cases (1:2 ratio). A hallmark feature of this phase ('transient synchronization') is that although the ESdC and HL-1 cells are functionally coupled, they still maintain their endogenous frequencies.

As co-culture continues, frequency synchronization progresses and a persistent 1:2 ratio of coupling is observed (Fig. 1A (iii)). This transitions (after 35 min) into a 1:1 AP synchronization (Fig. 1A (iv)) between HL-1 cells and ESdC. At this point, the delay of excitation between the two preparations remains constant (Fig. 2A; 30.3 min). Overall the data demonstrate that WT-ESdCs establish heterocellular coupling with HL-1 cells within 30 min of co-culture; however, during this time various degrees of frequency synchronization can be detected.

WT-ESdCs are not efficient in entraining spontaneously active preparations

To determine the likelihood of the ESdCs to gain pacemaker dominance, we examined the spontaneous activity, origin of excitation and conduction velocity in 31 co-cultures 15 hours after transplantation. A transmitted light image documented the position of the ESdCs on the MEA electrode field (Fig. 3Aa, Ba). In 91 % of the co-cultures, ESdCs had established synchronized electrical activity with the HL-1 monolayer (n = 31; Fig. 4A). The coupling was characterized by **i.** simultaneous contractions of the HL-1 cells and the ESdCs, and **ii.** synchronized FP activity in the HL-1 monolayer (Fig. 3Ac, Bc; location 2) and in the location of the ESdCs (location 1). As previously described, the FP underneath the ESdCs was characterized by two negative peaks that derived from the sequential activation of the HL-1 monolayer and the ESdCs on the same MEA electrode (Fig. 3Ad).

In our *in vitro* pacemaker model, the spontaneously active ESdCs compete with the spontaneously active HL-1 monolayer for pacemaker dominance. Under these circumstances, only 13 % of the WT-ESdCs in electrically coupled WT-ESdC/HL-1 cultures obtained pacemaker dominance (Fig. 4B). In the remaining 86 %, HL-1 cells resumed dominant pacemaker activity and the WT-ESdCs followed. The ESdCs were considered the origin of excitation **i.** when the MEA electrode underneath the ESdCs was the earliest site of excitation (Fig. 3Ba, Bb) and **ii.** when the beating frequency recorded reflected the endogenous frequency of the ESdCs. The frequency of HL-1 cells and ESdCs respectively remained uninfluenced by the co-culture (Fig. S2A). Representative examples are presented in Fig. 3AB. Control experiments revealed a 100 % success rate of the ESdC to obtain pacemaker dominance when they were plated on quiescent HL-1 monolayers (Fig. 4B). Our data demonstrate that WT-ESdCs can establish intercellular coupling with cardiac host tissue however, their effectiveness in obtaining pacemaker dominance is limited in spontaneously active preparations.

Cx43(−/−)-ESdCs are the better pacemakers

The intercellular conductance between SAN cardiomyocytes is low in comparison to atrial or ventricular cardiomyocytes [7,8] and Cx43 expression is absent. We determined by immunoblotting and immunostaining the presence of cardiac connexins in ESdCs and HL-1 cells. ESdCs as well as HL-1 cells tested positive for the expression of Cx40, Cx43 and Cx45 (Fig. 5) [14,21,28]. Expression of Cx30.2 a connexin described in the mouse SAN and conduction system [8,26] was not detected in WT- or Cx43(−/−)-ESdCs by immunostaining (data not shown [26]). To test the hypothesis that a more SAN-like expression pattern of connexin isoforms increases the success of biological pacemakers to assume and maintain pacemaker dominance, we used ESdCs derived from ESCs deficient in the expression of Cx43 [13,29]. Cx43(−/−)-ESdCs do not seem to have a compensatory upregulation of Cx45 or Cx40 respectively (Fig. 5).

Cx43(−/−)-ESdCs were transplanted onto spontaneously active HL-1 monolayers and the change in the spontaneous activity of the two preparations was monitored after 15 hrs of co-culture. Analysis of the electrical activity on MEAs revealed that 86 % of Cx43(−/−)-ESdCs (n = 30; Fig. 4A) established heterocellular coupling to HL-1 monolayers and obtained pacemaker dominance in 40 % of the hetero-cellular cultures (Fig. 4B). Also Cx43(−/−)-ESdCs achieved pacemaker dominance at 100 % when transplanted onto quiescent HL-1 cultures.

To compare how the lack of Cx43 effects the heterocellular coupling between WT- or Cx43 (−/−)-ESdCs and HL-1 monolayers, we categorized the time from the onset of co-culture until a 1:1 coupling ratio into 3 phases. The ‘unsynchronized’ phase starts at the onset of co-culture and lasts as long as the beating frequencies of the ESdCs and HL-1 cells remain independent of each other. The following phase of ‘transient synchronization’ describes the period where both preparations maintain their individual beating frequencies but periods of synchronization can be observed. During the ‘partial conduction block’, one of the preparations has lost its endogenous beating rhythm but no 1:1 coupling ratio is yet achieved. In co-cultures with Cx43 (−/−)-ESdCs, the entire time course of heterocellular coupling was significantly prolonged (unsynchronized: 4.73 ± 1.39 hr; ‘transient coupling’: 0.57 ± 0.18 hr; ‘partial conduction block’: 5.4 ± 0.9 hr; Fig. 4C). The data indicate that the reduced intercellular coupling within the Cx43(−/−)-ESdCs prolongs their time to establish intercellular coupling with the HL-1 monolayer.

Differences between WT- and Cx43(−/−)-ESdCs

It was demonstrated that aggregate size plays a significant role in its ability to pace an adult cardiomyocyte [30], therefore we determined the size of the ESdCs transplanted. Three dimensional ESdC aggregates grow out and flatten after attaching to the HL-1 monolayer. Assuming that differences in the aggregates diameters would manifest itself in an increased area of contact with the HL-1 monolayer after attaching, we determined the diameter of the attached ESdCs. WT-ESdCs diameter ranged from 242 to 409 μm^2 and Cx43(−/−)-ESdCs diameter ranged from 253 to 396 μm^2. No significant difference was determined in aggregate size nor was there a correlation between the success of becoming a dominant pacemaker and the size of the ESdC aggregate transplanted (Fig. S2).

ESdCs undergo *in vitro* differentiation and therefore the expression of ion and gap junction channels changes with time in culture [13,28]. Neither the time course of differentiation determined by the change in ISI (Fig. S3) nor the spontaneous beating frequency at day 14–18 of differentiation (WT-ESdCs: 1.25 ± 0.2 Hz; n = 4; Cx43(−/−)-ESdC: 1.1 ± 0.3 Hz; n = 11), or the resting membrane potential of WT- and Cx43(−/−)-ESdCs exhibited significant differences (WT: −64 ± 1.6 mV; n=4; Cx43(−/−): −62.0 ± 1.5 mV; n=5) [13]. These data

suggest that the increased success of Cx43(−/−)-ESdCs is not due to differences in its aggregate size or their electrophysiological properties.

To determine how the lack of Cx43 changes the intercellular resistance between ESdCs we performed double whole cell voltage clamp (DWVC) experiments on ESdC cell pairs [31], and measured the conduction velocity (θ) in ESdCs. The intercellular conductance was significantly decreased in Cx43(−/−)-ESdCs (WT-ESdCs: 14.8 nS, n = 4; vs. Cx43(−/−)-ESdCs: 1.2 nS; n = 3; Fig. S3) and coincided with a significantly decreased θ of Cx43(−/−)-ESdCs (1.25 ± 0.4 cm/s; n = 5 cultures) in comparison to WT-ESdC (2.2 ± 0.2 cm/s; n = 6 cultures) [13].

Also the interaction between Cx43(−/−)-ESdCs and HL-1 monolayers was affected by the lack of Cx43 expression. Both the WT- and Cx43(−/−)- ESdCs affected the excitation spread within the HL-1 monolayer by acting as a current sink. In HL-1 monolayers a stable and reproducible θ of 2.1 ± 0.4 cm/s (n = 70 cultures) was observed. This θ was unchanged (2.2 ± 0.4 cm/s; n = 54) in co-cultures, in areas distant from the ESdCs. However, thetas; in the HL-1 monolayer decreased significantly when the excitation wavefront approached the area underneath the ESdCs (Fig. 6AB). In HL-1 and WT-ESdC co-cultures, a 50 % decrease of the normalized θ could be detected (Fig. 6CD). In HL-1 and Cx43(−/−)-ESdC co-cultures however, the reduction of θ amounted to only 25 % (1.7 ± 0.3 cm/s, n = 10; Fig. 6D). The reduced intercellular conductance between Cx43(−/−)-ESdCs supports the hypothesis that it presents less of a current sink to the HL-1 monolayer.

Biased action potential propagation from the ESdCs into the HL-1 cells

It is a matter of controversy whether the spatially defined expression of Cx45 and Cx30.2 in the SAN and Cx40 and Cx43 in the atrial cardiomyocytes could favor the pacemaker dominance of the SAN by the formation of rectifying, heterotypic gap junction channels. To determine if the lack of Cx43 biases AP propagation between the HL-1 monolayer and the ESdCs in either direction, we analyzed the degree of frequency synchronization in co-cultures where either WT- or Cx43(−/−)-ESdCs were pacemakers or the HL-1 monolayers were pacemakers. The analysis was in all cases performed 15 hrs after co-culture was established. In preparations where WT- or Cx43(−/−)-ESdCs were pacemakers, every AP propagated from the ESdCs into the HL-1 monolayer (ratio of 1:1). However, in preparations where the HL-1 monolayers were the pacemakers, a 1:1 ratio of AP propagation from the HL-1 monolayer into the ESdCs occurred in only 21 of 31 co-cultures with WT-ESdCs and 14 of 28 co-cultures with Cx43(−/−)-ESdCs (Fig. 7C). The degree of conduction block varied. Figure 7 shows examples of a 1:2 (A) and 1:3 (B) ratio of AP synchronization. FPs recorded from electrodes underneath the HL-1 cells (2) (Aa, Ba) appear at the characteristic HL-1 frequency, FPs from the electrode underneath the ESdCs (1) (Ab, Bb) exhibit a double peak representing the sequential excitation of HL-1 cells and ESdCs. The larger HL-1 signals on location (1) and (2) are synchronized whereas the smaller ESdC signal (arrow) appears only at a 1:2 (Ab) or 1:3 ratio (Bb) upon HL-1 cell excitation. The data indicate that excitation spread is hindered from the HL-1 cells into ESdCs with a more pronounced block in the Cx43(−/−)-ESdCs.

Discussion

Our experiments demonstrate that ESdCs can function as biological pacemakers in spontaneously active cardiomyocyte preparations and that the expression of the major cardiac gap junction isoform, Cx43, is not necessary to establish intercellular coupling with the host cardiac tissue. On the contrary, we demonstrate that ESdCs deficient for the expression of Cx43 obtained pacemaker dominance at a three fold higher rate. Our data support the notion that this improvement is based on the increased intercellular resistance within this biological pacemaker. This change in intercellular coupling is of critical importance **i.** during the phase

of pacemaker capture where the Cx43(−/−)-ESdC can maintain its independent beating frequency while intercellular coupling is already established and **ii.** in coupled preparations where arrhythmic HL-1 excitations are less likely to propagate into the Cx43(−/−)-ESdCs.

Underdrive

ESdCs can obtain pacemaker dominance in the heart after endogenous pacemakers are ablated [2,3] and *in vitro* we showed that ESdCs can even gain pacemaker dominance when the host preparation is spontaneously active. When two spontaneously active cells with different endogenous beating frequencies establish intercellular coupling their shared spontaneous activity becomes more comparable to the faster beating cell [32,33] since the shorter cycle length of the faster cell allows it to induce an escape beat and gain pacemaker dominance [34]. Consequently it is not surprising that in our model 87 % of the co-cultures adopted the faster beating frequency of the HL-1 monolayers (Fig. 5A). However, in contrast to previous studies, the WT-ESdCs gained pacemaker dominance in 13 % of the preparation in spite of its 4 times slower endogenous frequency. In addition to underdrive, ESdCs may have attained pacemaker dominance simply due to loss of spontaneous activity in the HL-1 monolayers. However, in this case the likelihood for WT- and Cx43(−/−)-ESdCs would be the same as demonstrated in ours (Fig. 4B) and previously published experiments [2,3]. It further has to be considered that the ESdCs did not become the pacemakers, but rather heterocellular interactions promoted the origin of excitation to move underneath the ESdCs while still originating from the HL-1 monolayer. This could be induced e.g. by mechanical stimulation of the HL-1 monolayer through the ESdCs contractions. However, also in this case, no difference in the success rate should appear between WT- and Cx43(−/−)-ESdCs given that they beat at comparable beating frequencies. In addition the uncoupling of the electrical excitation from the contraction by butanedione monoxime treatment [2,3], also the block of stretch activated ion channels by streptomycin (data not shown) remained without effect on the pacemaker dominance of the ESdCs. Further mechanisms by which the ESdCs could change the HL-1 cells excitability are the heterocellular, electrotonic interaction, or the heterocellular exchange of second messenger molecules (e.g. calcium, cAMP or $InsP_3$). These mechanisms would strongly depend on the intercellular resistance established within the ESdCs and between the HL-1 monolayers and the ESdCs. Consequently an increased likelihood of success would be expected for the WT-ESdC.

In other preparations the electrotonic interaction between two cells with different resting membrane potentials was shown to have a significant effect on the frequency of synchronization. Nevertheless in our *in vitro* model it seems to be of reduced relevance since the spontaneous activity of neither preparation is modulated by the co-culture conditions.

When a pacemaker with a slower endogenous beating frequency captures and drives a faster beating preparation, it is described as ‘underdrive’. Underdrive of cardiac preparations was reported to have a low rate of success [35,36] and it is not fully understood how it is established electrophysiologically. It is not the aim of this paper to solve this conundrum, but it is known that a pacemaker cycle can be disrupted by premature stimuli. Depending on the point of time when these stimuli interrupt the excitation cycle, they can delay, abbreviate, or even annihilate the spontaneous activity [37–40]. Although obviously the biological pacemaker ‘of choice’ would have an endogenous beating frequency within the physiological range of the host organ, our model system provides important insight on parameters that could help to design biological pacemakers that gain and maintain their function even when arrhythmic challenges occur.

Differences between WT- and Cx43(−/−)-ESdCs

Our experiments show that Cx43(−/−)-ESdCs gain pacemaker dominance over HL-1 monolayers at a significantly higher rate than WT-ESdCs. We ruled out differences in the WT-

and Cx43(−/−)-ESdCs size, beating frequency, and membrane potential. Either parameter could render an advantage to one of the pacemaker aggregates if capture depended on the liminal area of excitation, over-drive, or on changing the HL-1 cells' V_m [41]. A paper by de Boer et al. [30] nicely showed *in silico* that at low coupling resistance and low cell number, pacing success of a quiescent cell linearly depends on the cluster size of the pacing cardiomyocytes, and the heterocellular conductance established. Once a certain aggregate size is reached however, the major determinant for success is the intercellular conductance. The independence of the success of the ESdC pacemaker from the aggregate size in our model potentially indicates that all aggregates used exceeded the critical size needed to induce action potential propagation in the HL-1 monolayer.

The SAN is not a uniform structure but its volume can contain up to 65 % of non-excitable cells such as fibroblasts. In a previous study of this laboratory, it was determined that fibroblasts increase the beating frequency variability in cardiomyocyte/fibroblast co-cultures [18]. This was shown to be true not only in monolayers but also in three dimensional aggregates of ESdCs. Given the heterogeneity of the SAN, we chose a biological pacemaker preparation that also contains myocytes and other non-excitable cells. The beating frequency as well as the beating frequency variability were not significantly different between WT- and Cx43(−/−)-ESdC preparations. This suggest that WT- and Cx43(−/−)-ESdC aggregates contain a similar proportion of non-ESdCs and excludes that a difference in the heterocellular composition of the Cx43(−/−)-ESdCs played a role in their increased success rate.

In HL-1 cells we identified the expression of the cardiac connexins Cx30.2 (not shown), Cx40, Cx43, and Cx45 [18]. In WT-ESdCs Cx40, Cx43 and Cx45 could be detected. It was shown previously that ESdCs are initially coupled by Cx45 and that Cx43 as well as Cx40 are up-regulated with further maturation of the ESdCs [13,15,28]. Cx43(−/−)-ESdCs have an increased intercellular resistance and no compensatory change in the expression levels of other cardiac connexins; also the lack of Cx43 did not change the time course of ESdC differentiation [13]. WT- and Cx43(−/−)-ESdCs both established sufficient intercellular coupling with HL-1 monolayers to allow for frequency synchronization most likely by heteromeric and/or heterotypic gap junction channel formation at the site of heterocellular contact [12,42,43].

A high intercellular resistance within the SAN and the formation of heterotypic gap junctions at the interface of the SAN and the atrial tissue is discussed to prevent hyperpolarization of the pacemaker and back propagation of APs from the atrial myocytes into the pacemaker region respectively. In our preparations Cx43(−/−)-ESdCs exhibit a higher intercellular resistance. The increased chance of conduction block from the HL-1 monolayers to the Cx43(−/−)-ESdC could support that voltage dependent rectification occurs. However, further explanations are a current source to sink mismatch at the branching point from the HL-1 monolayer into the 3D-ESdC (Fig. 7) [44] or an increased heterocellular resistance between HL-1 cells and Cx43 (−/−)-ESdCs that prevents AP propagation. Although in the latter case propagation block should be observed into and out of the pacemaker aggregate. We can not rule out that voltage dependent rectification at the gap junction level occurs between Cx43(−/−)-ESdCs and HL-1 cells. This as well as the heterocellular resistance would need to be confirmed with DWVC experiments in heterocellular HL-1/ESdC cell pairs in future studies.

Summary

Our data demonstrate that ESdCs can serve as biological pacemaker in spontaneously active cardiomyocyte preparations. The spontaneous activity of the host tissue in our model system mimics the physiological condition where a biological pacemaker would compete for pacemaker dominance with the excitable, potentially arrhythmic host tissue. The back drop of our model is that the ESdCs have to underdrive the HL-1 monolayer to gain pacemaker

dominance. This leads us to underestimate the success rate of both WT- and Cx43(−/−)-ESdCs given that both preparations gain pacemaker dominance at 100 % in quiescent HL-1 monolayers. Overall, we are the first to demonstrate that a modification of the connexin isoform expression in the ESdCs towards a more SAN phenotype, namely an increased intercellular resistance within the pacemaker, significantly increases the success rate of pacemaker dominance. Further optimization of intercellular coupling in biological pacemakers e.g. by establishing rectifying coupling with the host tissue, will increase their potential to obtain pacemaker dominance in spontaneously active preparations and withstand overdrive from ectopic arrhythmic activity.

Supplementary Material

Refer to Web version on PubMed Central for supplementary material.

Acknowledgements

The authors want to thank Dr. W. C. Claycomb (LSU, New Orleans, LA) for providing the HL-1 cells and Dr. N. Kumar (UIC, Chicago, IL) for providing the Cx30.2 antibody. This work was supported by grants from the American Heart Association (AHA0610110Z to JPF; AHA0330393Z to KB), the Potts Foundation Loyola University Chicago (RFC 11086), and the NIH (R01 HL89617 to KB).

References

1. Ruhparwar A, Tebbenjohanns J, Niehaus M, Mengel M, Irtel T, Kofidis T, et al. Transplanted fetal cardiomyocytes as cardiac pacemaker. Eur J Cardiothorac Surg 2002;21(5):853–858. [PubMed: 12062274]
2. Xue T, Cho HC, Akar FG, Tsang SY, Jones SP, Marban E, et al. Functional integration of electrically active cardiac derivatives from genetically engineered human embryonic stem cells with quiescent recipient ventricular cardiomyocytes: insights into the development of cell-based pacemakers. Circulation 2005;111(1):11–20. [PubMed: 15611367]
3. Kehat I, Khimovich L, Caspi O, Gepstein A, Shofti R, Arbel G, et al. Electromechanical integration of cardiomyocytes derived from human embryonic stem cells. Nat Biotechnol 2004;22(10):1282–1289. [PubMed: 15448703]
4. Verheule S, van Kempen MJ, Postma S, Rook MB, Jongsma HJ. Gap junctions in the rabbit sinoatrial node. Am J Physiol Heart Circ Physiol 2001;280(5):H2103–H2109. [PubMed: 11299212]
5. Verheijck EE, Wessels A, van Ginneken AC, Bourier J, Markman MW, Vermeulen JL, et al. Distribution of atrial and nodal cells within the rabbit sinoatrial node: models of sinoatrial transition. Circulation 1998;97(16):1623–1631. [PubMed: 9593568]
6. Verheijck EE, van Kempen MJ, Veereschild M, Lurvink J, Jongsma HJ, Bouman LN. Electrophysiological features of the mouse sinoatrial node in relation to connexin distribution. Cardiovasc Res 2001;52(1):40–50. [PubMed: 11557232]
7. Coppen SR, Severs NJ, Gourdie RG. Connexin45 (alpha 6) expression delineates an extended conduction system in the embryonic and mature rodent heart. Dev Genet 1999;24(1–2):82–90. [PubMed: 10079513]
8. Kreuzberg MM, Sohl G, Kim JS, Verselis VK, Willecke K, Bukauskas FF. Functional properties of mouse connexin30.2 expressed in the conduction system of the heart. Circ Res 2005;96(11):1169–1177. [PubMed: 15879306]
9. Kurata Y, Matsuda H, Hisatome I, Shibamoto T. Effects of pacemaker currents on creation and modulation of human ventricular pacemaker: theoretical study with application to biological pacemaker engineering. Am J Physiol Heart Circ Physiol 2007;292(1):H701–718. [PubMed: 16997892]
10. Boyett MR, Dobrzynski H, Lancaster MK, Jones SA, Honjo H, Kodama I. Sophisticated architecture is required for the sinoatrial node to perform its normal pacemaker function. J Cardiovasc Electrophysiol 2003;14(1):104–106. [PubMed: 12625620]

11. Joyner RW, Kumar R, Golod DA, Wilders R, Jongsma HJ, Verheijck EE, et al. Electrical interactions between a rabbit atrial cell and a nodal cell model. Am J Physiol Heart Circ Physiol 1998;274 (6):H2152–H2162.
12. Valiunas V, Weingart R, Brink PR. Formation of heterotypic gap junction channels by connexins 40 and 43. Circ Res 2000;86(2):E42–E49. [PubMed: 10666425]
13. Banach K, Halbach MD, Hu P, Hescheler J, Egert U. Development of electrical activity in cardiac myocyte aggregates derived from mouse embryonic stem cells. Am J Physiol Heart Circ Physiol 2003;284(6):H2114–H2123. [PubMed: 12573993]
14. Boheler KR, Czyz J, Tweedie D, Yang HT, Anisimov SV, Wobus AM. Differentiation of pluripotent embryonic stem cells into cardiomyocytes. Circ Res 2002;91(3):189–201. [PubMed: 12169644]
15. Egashira K, Nishii K, Nakamura K, Kumai M, Morimoto S, Shibata Y. Conduction abnormality in gap junction protein connexin45-deficient embryonic stem cell-derived cardiac myocytes. Anat Rec A Discov Mol Cell Evol Biol 2004;280(2):973–979. [PubMed: 15372487]
16. Claycomb WC, Lanson NA Jr, Stallworth BS, Egeland DB, Delcarpio JB, Bahinski A, et al. HL-1 cells: a cardiac muscle cell line that contracts and retains phenotypic characteristics of the adult cardiomyocyte. Proc Natl Acad Sci 1998;95(6):2979–2984. [PubMed: 9501201]
17. White SM, Constantin PE, Claycomb WC. Cardiac physiology at the cellular level: use of cultured HL-1 cardiomyocytes for studies of cardiac muscle cell structure and function. Am J Physiol Heart Circ Physiol 2004;286(3):H823–829. [PubMed: 14766671]
18. Fahrenbach JP, Mejia-Alvarez R, Banach K. The relevance of non-excitable cells for cardiac pacemaker function. J Physiol 2007;585(Pt 2):565–578. [PubMed: 17932143]
19. Burstein B, Qi XY, Yeh YH, Calderone A, Nattel S. Atrial cardiomyocyte tachycardia alters cardiac fibroblast function: A novel consideration in atrial remodeling. Cardiovasc Res 2007;76(3):442–452. [PubMed: 17720149]
20. Nagy A, Rossant J, Nagy R, Abramow-Newerly W, Roder JC. Derivation of completely cell culture-derived mice from early-passage embryonic stem cells. Proc Natl Acad Sci 1993;90(18):8424–8428. [PubMed: 8378314]
21. Oyamada Y, Komatsu K, Kimura H, Mori M, Oyamada M. Differential regulation of gap junction protein (connexin) genes during cardiomyocytic differentiation of mouse embryonic stem cells in vitro. Exp Cell Res 1996;229(2):318–326. [PubMed: 8986615]
22. Hescheler J, Wartenberg M, Fleischmann BK, Banach K, Acker H, Sauer H. Embryonic stem cells as a model for the physiological analysis of the cardiovascular system. Methods Mol Biol 2002;185:169–187. [PubMed: 11768987]
23. Halbach M, Egert U, Hescheler J, Banach K. Estimation of action potential changes from field potential recordings in multicellular mouse cardiac myocyte cultures. Cell Physiol Biochem 2003;13 (5):271. [PubMed: 14586171]
24. Egert U, Knott T, Schwarz C, Nawrot M, Brandt A, Rotter S, et al. MEA-Tools: an open source toolbox for the analysis of multi-electrode data with MATLAB. J Neurosci Methods 2002;117(1): 33–42. [PubMed: 12084562]
25. Ai X, Pogwizd SM. Connexin 43 downregulation and dephosphorylation in nonischemic heart failure is associated with enhanced colocalized protein phosphatase type 2A. Circ Res 2005;96(1):54–63. [PubMed: 15576650]
26. Nielsen PA, Kumar NM. Differences in expression patterns between mouse connexin-30.2 (Cx30.2) and its putative human orthologue, connexin-31.9. FEBS Lett 2003;540(1–3):151–156. [PubMed: 12681499]
27. Kapur N, Banach K. Inositol-1,4,5-trisphosphate-mediated spontaneous activity in mouse embryonic stem cell-derived cardiomyocytes. J Physiol 2007;581(Pt 3):1113–1127. [PubMed: 17379641]
28. Van Kempen M, Van Ginneken A, De GI, Mutsaers N, Opthof T, Jongsma H, et al. Expression of the electrophysiological system during murine embryonic stem cell cardiac differentiation. Cell Physiol Biochem 2003;13(5):263–270. [PubMed: 14586170]
29. Reaume AG, De Sousa PA, Kulkarni S, Langille BL, Zhu D, Davies TC, et al. Cardiac malformation in neonatal mice lacking connexin43. Science 1995;267(5205):1831–1834. [PubMed: 7892609]

30. de Boer TP, van der Heyden MA, Rook MB, Wilders R, Broekstra R, Kok B, et al. Pro-arrhythmogenic potential of immature cardiomyocytes is triggered by low coupling and cluster size. Cardiovasc Res 2006;71(4):704–714. [PubMed: 16824499]

31. Banach K, Weingart R. Voltage gating of Cx43 gap junction channels involves fast and slow current transitions. Pflugers Arch 2000;439(3):248–250. [PubMed: 10650974]

32. Michaels DC, Matyas EP, Jalife J. Dynamic interactions and mutual synchronization of sinoatrial node pacemaker cells. A mathematical model. Circ Res 1986;58(5):706–720. [PubMed: 3708767]

33. Ypey DL, VanMeerwijk WP, Ince C, Groos G. Mutual entrainment of two pacemaker cells. A study with an electronic parallel conductance model. J Theor Biol 1980;86(4):731–755. [PubMed: 7253669]

34. Ypey DL, Clapham DE, DeHaan RL. Development of electrical coupling and action potential synchrony between paired aggregates of embryonic heart cells. J Membr Biol 1979;51(1):75–96. [PubMed: 522130]

35. Altamura G, Bianconi L, Toscano S, Lo Bianco F, Jesi AP, Pistolese M. Transcutaneous cardiac pacing for termination of tachyarrhythmias. Pacing Clin Electrophysiol 1990;13(12 Pt 2):2026–2030. [PubMed: 1704587]

36. Loeb JM, Murdock DK, Randall WC, Euler DE. Supraventricular pacemaker underdrive in the absence of sinus nodal influences in the conscious dog. Circ Res 1979;44(3):329–334. [PubMed: 761314]

37. Anumonwo JM, Delmar M, Vinet A, Michaels DC, Jalife J. Phase resetting and entrainment of pacemaker activity in single sinus nodal cells. Circ Res 1991;68(4):1138–1153. [PubMed: 2009613]

38. Clay JR, Guevara MR, Shrier A. Phase resetting of the rhythmic activity of embryonic heart cell aggregates. Experiment and theory. Biophys J 1984;45(4):699–714. [PubMed: 6722263]

39. Jalife J, Antzelevitch C. Phase resetting and annihilation of pacemaker activity in cardiac tissue. Science 1979;206(4419):695–697. [PubMed: 493975]

40. Shrier A, Clay JR, Brochu RM. Effects of tetrodotoxin on heart cell aggregates. Phase resetting and annihilation of activity. Biophys J 1990;58(3):623–629. [PubMed: 2207254]

41. Lindemans FW, Denier Van der Gon JJ. Current thresholds and liminal size in excitation of heart muscle. Cardiovasc Res 1978;12(8):477–485. [PubMed: 719660]

42. Burt JM, Fletcher AM, Steele TD, Wu Y, Cottrell GT, Kurjiaka DT. Alteration of Cx43:Cx40 expression ratio in A7r5 cells. Am J Physiol Cell Physiol 2001;280(3):C500–C508. [PubMed: 11171569]

43. Valiunas V, Gemel J, Brink PR, Beyer EC. Gap junction channels formed by coexpressed connexin40 and connexin43. Am J Physiol Heart Circ Physiol 2001;281(4):H1675–H1689. [PubMed: 11557558]

44. Kucera JP, Kleber AG, Rohr S. Slow conduction in cardiac tissue, II: effects of branching tissue geometry. Circ Res 1998;83(8):795–805. [PubMed: 9776726]

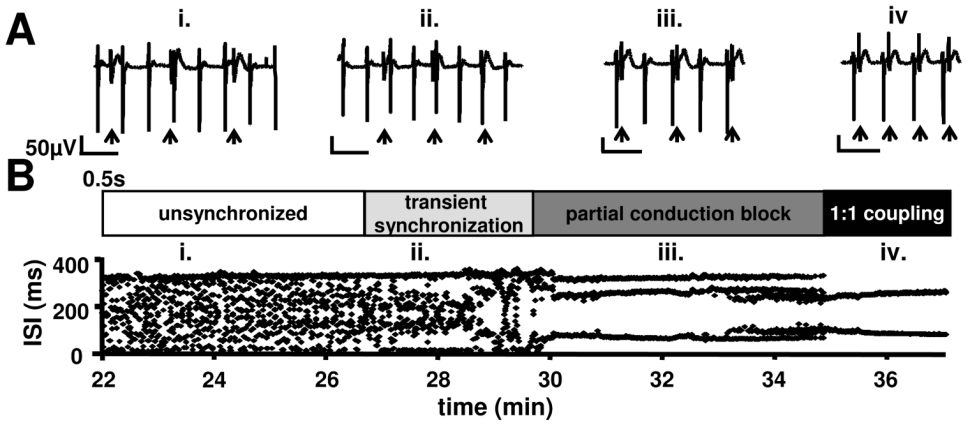

Figure 1. Onset of electrical synchronization between ESdC and HL-1 cells

(**A**) FP signals from an electrode located underneath the ESdC aggregate which is attached to the HL-1 monolayer. ESdC (small amplitude; arrow) and HL-1 (large amplitude) induced FP spikes can be detected. (**B**) ISIs between all spikes (ESdC and HL-1) (recorded on the electrode shown in **A**) are plotted as a function of time. Different phases of ESdC and HL-1 synchronization are detected. HL-1 and ESdC activities are independent (**i**), transiently synchronized (**ii**), synchronized at non-1:1 ratios (**iii**), or synchronized for each beat (1:1 ratio; **iv**).

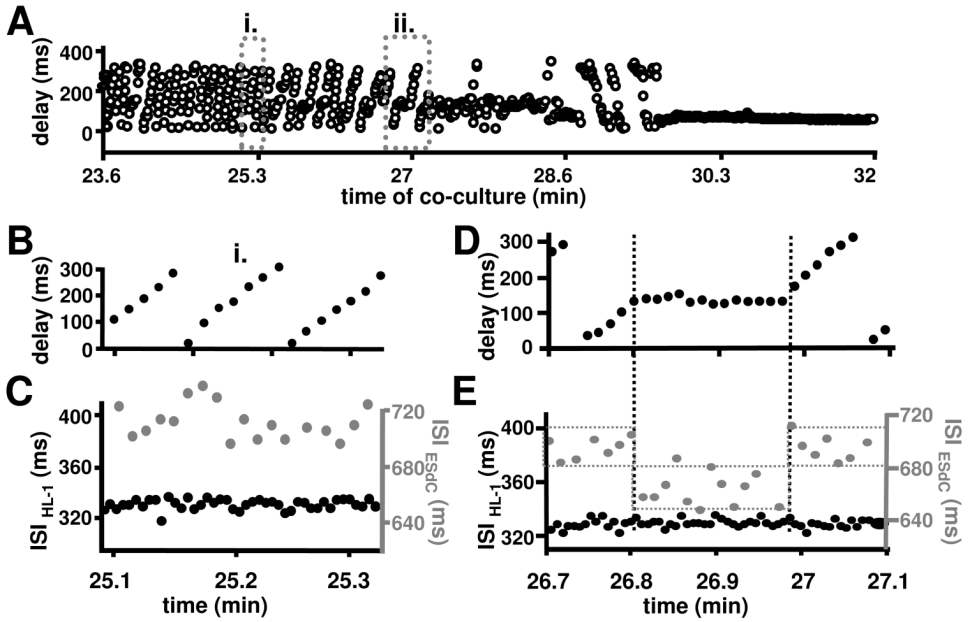

Figure 2. Delay of AP propagation between HL-1 cells and ESdC

(**A**) For every excitation cycle of the HL-1 monolayer the delay between HL-1 and ESdC activity was determined during a period of independent activity (**i.**) and a period of transient synchronization (**ii.**). In **i**. the delay between HL-1 and ESdC activity is non-stationary (**B**). Separate analysis of the ESdCs and HL-1 spikes ISI revealed beating frequencies comparable to ESdCs and HL-1 cells in homocellular culture respectively (**C**). During transient synchronization (**ii**), the delay between the HL-1 cells and the ESdCs activity transiently stabilizes (**D**). At this point of time the ESdC's ISI is an integral value of the HL-1's ISI (**E**).

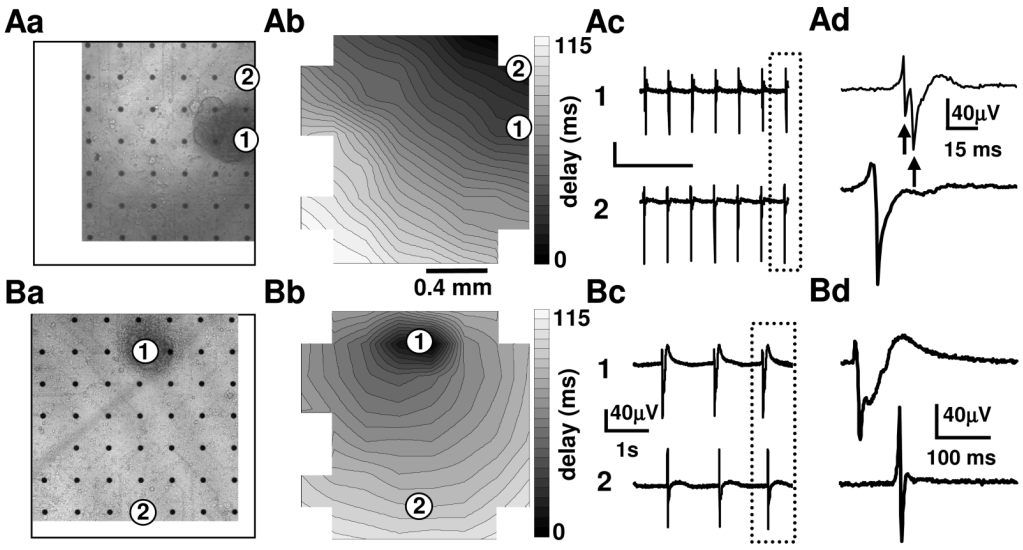

Figure 3. Electrical coupling between ESdC aggregates and HL-1 cells

Transmitted light photographs (**Aa, Ba**) of two MEA electrodes with HL-1 monolayers after the transplantation of WT-ESdCs. Contour plots reveal that excitation can originate in the HL-1 cells (**Ab**) as well as in the area of the transplanted WT-ESdC (**Bb**). The FPs recorded from the electrodes underneath the HL-1 monolayer only (2) and underneath the ESdC attached to the HL-1 monolayer (1) show synchronized activity (**Ac; Bc**). The FPs framed by the dotted line are shown at an increased time resolution. (**Ad**) The FP (1) shows a split signal (arrows) representing the subsequent excitation of the HL-1 monolayer and the WT-ESdC aggregate. When the ESdC is the origin of excitation, the two peaks are merged (Bd) to a prolonged FP rise time and ESdC/HL-1 activity can no longer be separated.

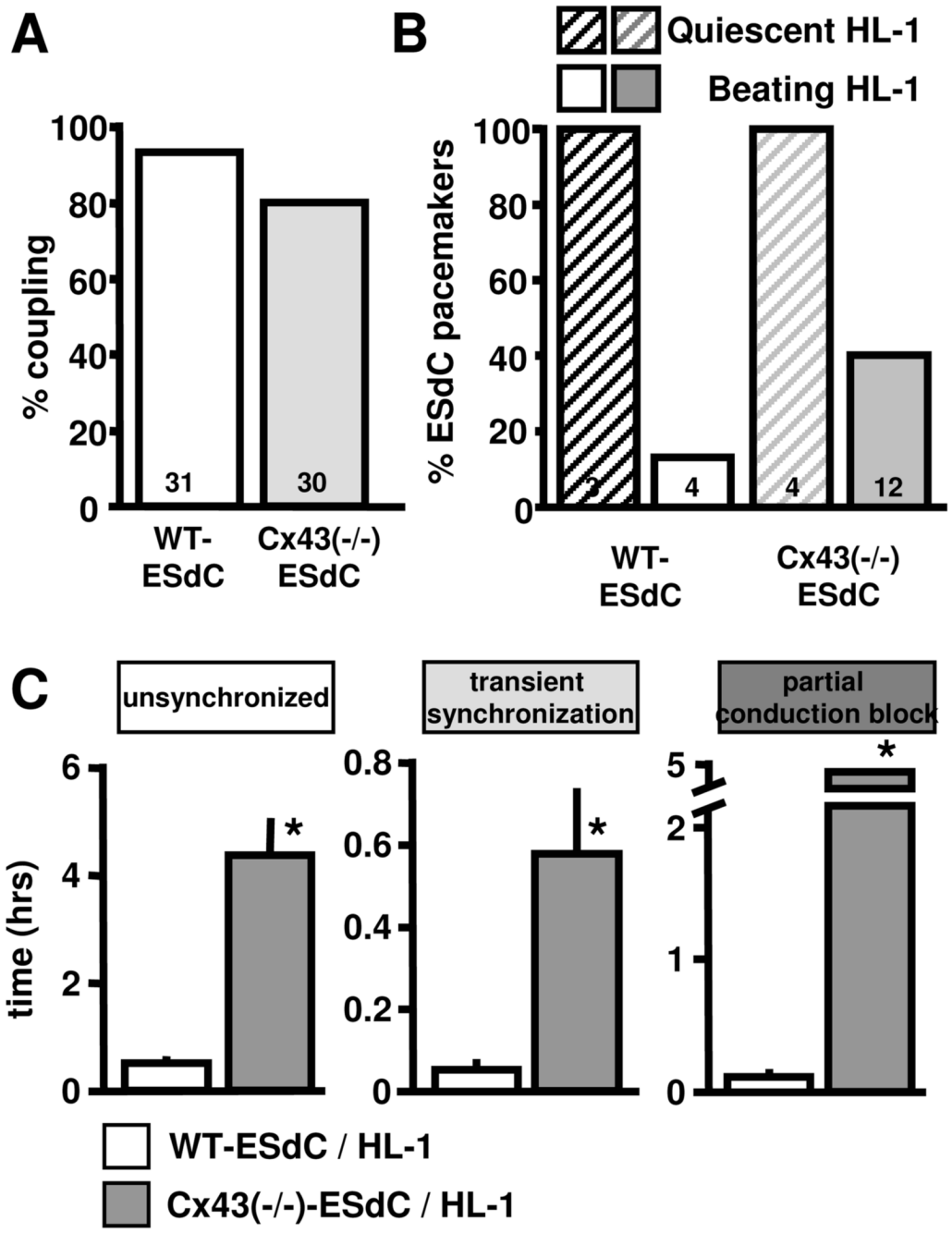

Figure 4. Cx43(−/−)-ESdCs make a better pacemaker

(**A**) Percentage of WT- and Cx43(−/−)-ESdCs that establish electrical coupling with HL-1 cells in co-culture. (**B**) Percentage of WT- and Cx43(−/−)-ESdCs that obtain pacemaker dominance when co-cultured with quiescent HL-1 monolayers (hatched bars), or spontaneously active HL-1 monolayers (filled bars). Cx43(−/−)-ESdC are more likely gain pacemaker dominance over spontaneously active HL-1 monolayers (40 % vs. 13 %). (**C**) Comparison of the time that it takes for WT- (white) and Cx43(−/−)-ESdCs (grey) to establish intercellular coupling with HL-1 monolayers. Cx43(−/−)-ESdC reside significantly longer in the phases of unsynchronized, transiently coupled, and partial conduction block activity.

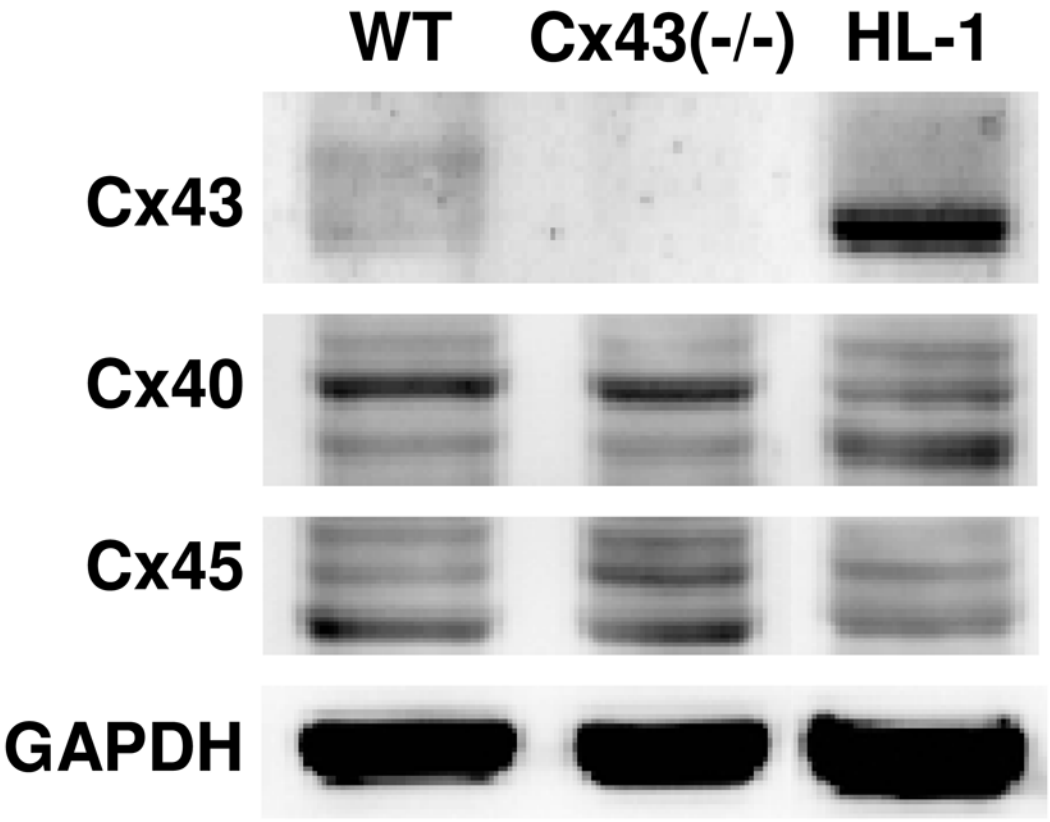

Figure 5. Connexin expression in HL-1 cells and ESdCs

(**A**) Immunoblots for Cx40, Cx43, and Cx45 in WT- and Cx43(−/−)-ESdCs and HL-1 cells. GAPDH was used as a loading control.

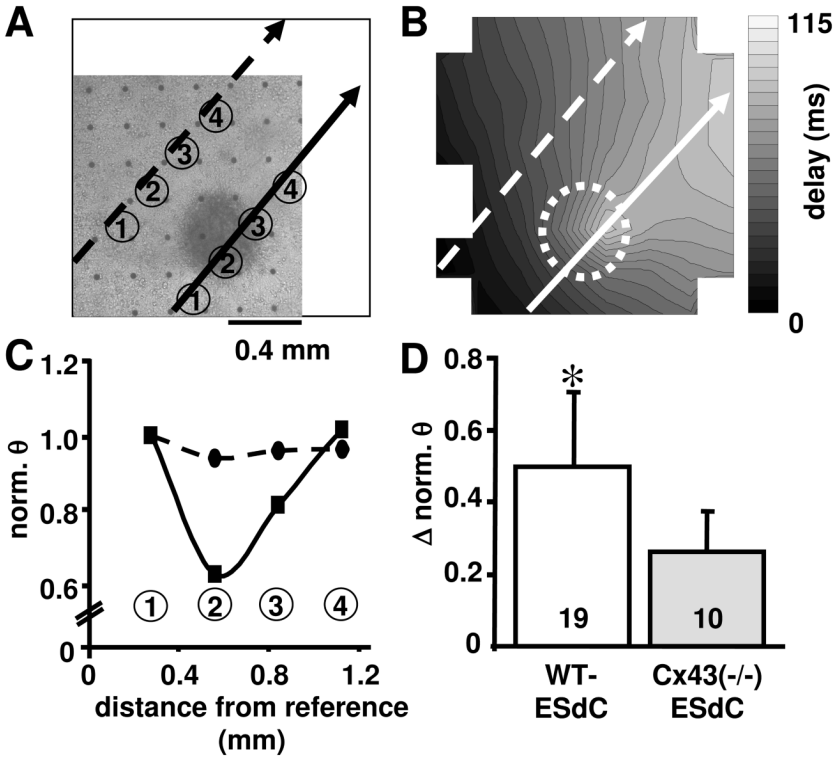

Figure 6. ESdCs act as a current sink for HL-1 monolayers

(**A**) Transmitted light image of HL-1/WT-ESdC co-culture on a MEA and the corresponding contour plot are shown (**B**; circle indicates position of the WT-ESdC). The conduction velocity (θ) through the HL-1 monolayer was analyzed along parallel paths distant from (dotted arrow) and underneath (solid arrow) the WT-ESdC. (**C**) Normalized θ along the two paths of excitation spread (electrodes are denounced by numbers) reflect a drop of θ at the location of the ESdC aggregate (position 2 solid arrow). (**D**) The summary (mean ± SD) of the ESdC aggregate induced reduction in θ was significantly larger in WT- (white) than in Cx43(−/−)-ESdC aggregates (grey). Number of experiments specified within the bar. * $P < 0.05$

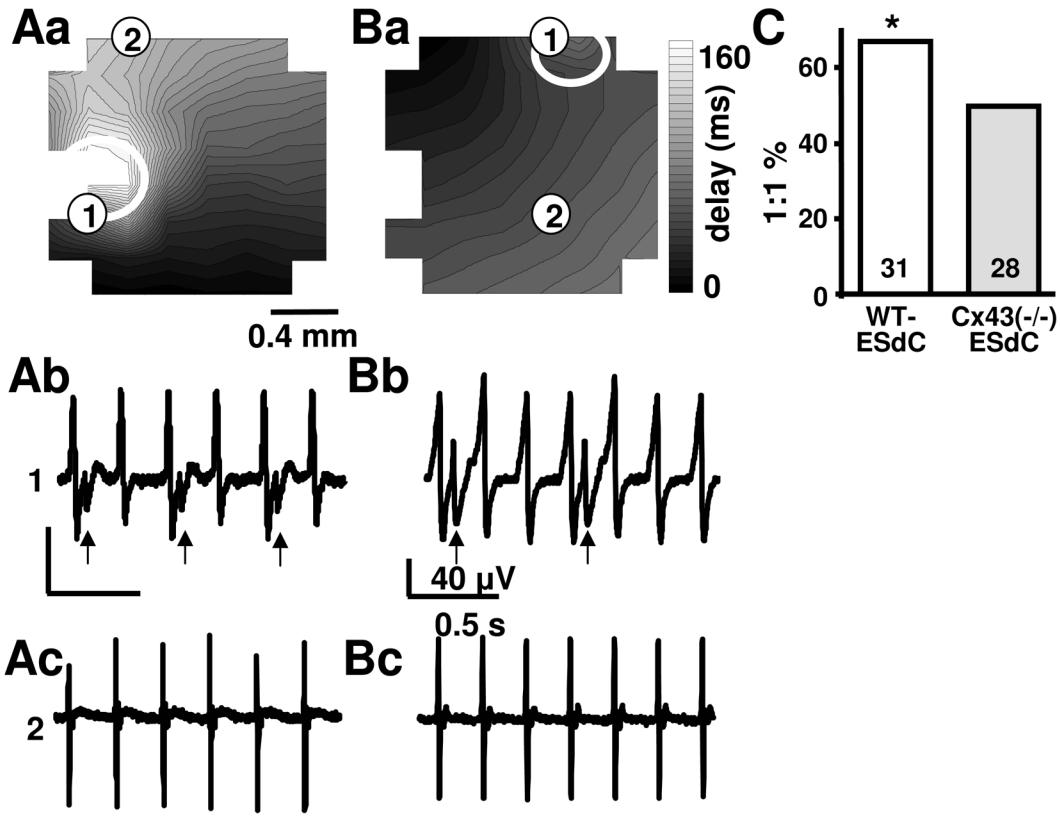

Figure 7. Biased excitation spread between HL-1 monolayers and ESdC aggregates

(**Aa, Ba**) Contour plots from two electrically coupled WT-ESdC/HL-1 co-cultures. The area of the ESdC is marked by the white circles. Representative FPs recorded from an electrode underneath the ESdC (**1: Ab, Bb**) and an electrode covered by only the HL-1 monolayer (**2: Ac, Bc**). The split FPs (arrows) occurs when APs propagate from the HL-1 monolayer into the ESdC. Excitation of both preparations can only be detected upon every second (**Ab**) or every third (**Bb**) HL-1 excitation cycle suggesting a hindered propagation from the HL-1 cells into the ESdC aggregates. (**C**) The summary of the experiments shows that in only 67 % of the WT- and 50 % of the Cx43(−/−)-ESdC and HL-1 co-cultures excitation was conducted at a 1:1 ratio from the HL-1 cells into the ESdCs. Number of experiments is specified within the bar; # P> 0.05